ZULFAQAR Journal of Defence Science, Engineering & Technology
e-ISSN: 2773-5281
Vol. 9, Issue 1 (2026)
DOI: https://doi.org/10.58247/jdset-2026-0901-02
Journal homepage: https://zulfaqarjdset.upnm.edu.my

MASS ATTENUATION COEFFICIENT, HALF–VALUE LAYER AND MEAN FREE PATH OF BISMUTH-BORO-TELLURITE GLASS USING PHY-X SOFTWARE

Nor Falihan Ramli[a, b], Azuraida Amat[b, *], Wan Yusmawati Wan Yusoff[b], Nurazlin Ahmad[b]

[a] Department of Defence Science, Faculty of Defence Science and Technology, National Defence University of Malaysia, Kem Sungai Besi, 57000 Kuala Lumpur, Malaysia
[b] Department of Physics, Centre for Defence Foundation Studies, National Defence University of Malaysia, Kem Sungai Besi, 57000 Kuala Lumpur, Malaysia

ARTICLE INFO

ARTICLE HISTORY
Received: 01-12-2025
Revised: 30-01-2026
Accepted: 01-04-2026
Published: 30-05-2026

KEYWORDS
Bismuth
Boro-Tellurite
Phy-X
Mass Attenuation Coefficient
Half Value Layer

ABSTRACT

A series of tellurite-based glasses with varying bismuth content was synthesized to investigate the influence of structural compactness on photon attenuation coefficient. The density of each composition was determined experimentally, whereas shielding parameters, including the mass attenuation coefficient (MAC), half-value layer (HVL), and mean free path (MFP), were evaluated at a photon energy of 0.662 MeV using established computational frameworks. According to the data, greater MAC values show that increasing glass density improves photon absorption. At the same time, the corresponding HVL and MFP values were reduced, indicating that photons require a shorter travel distance to be attenuated within the materials. The attenuation efficiency was found to depend strongly on density. Overall, the results demonstrate the increasing structural compactness enhances the intrinsic shielding capability of the tellurite glass system.

1.0 INTRODUCTION

Lead and concrete are represented of conventional radiation shielding materials that have a several limitations, such as toxicity, heavy weight, opacity, and lack of structural flexibility. Lead is very effective, but it can be harmful to the environment and human health. Concrete, on the other hand required large thickness and is opaque, which prevent it from being use in applications requiring visual monitoring. Due to this restriction, there is considerable industry need for lightweight, non-toxic, and optically transparent alternative shielding materials. these gaps are filled by glass-based shielding materials, which are appropriate for industrial, nuclear, and medical radiation. Glass-based radiation shielding materials have attracted sustained attention as promising alternatives to conventional lead-based barriers and concrete, owing to their combinations of high density, optical transparency, and mechanical properties [1-3]. Among the various glass formers, such as silicate, phosphate, and borate glasses have been explored for radiation shielding applications. Although silicate glasses have good chemical durability, but go through from relatively low density, limiting their shielding efficiency. Phosphate glasses have low melting temperature and have poor durable and chemical stable. Borate glasses possess excellent glass-forming ability but have poorer mechanical qualities and lower density. Compared to tellurite- and borate-containing systems offer low melting temperature, good thermal stability, and the ability to incorporate large amounts of heavy-metal oxide while preserving amorphous character [1, 4-5]. Boro-tellurite glass system represents a particularly attractive host matrix for shielding applications. Tellurite (TeO_2)-based glasses are characterized by relatively high density and favourable optical properties, while borate (B_2O_3) contribute structural flexibility and enhanced glass-forming ability. The combination of these two network formers enables fine control over physical characteristics including molar volume, oxygen packing density (OPD) and interatomic separation [6-8].

*Corresponding Author | Amat, A. | azuraida@upnm.edu.my

Boron exists in two primary coordination states within oxide glasses: trigonal BO_3 and tetrahedral BO_4 units [9]. Boro-tellurite (B_2O_3-TeO_2) glass constitute a particularly attractive host because the coexistence of trigonal and tetrahedral borate units with tellurite and tellurate groups affords flexible structure networks with high refractive index, broad transmission windows, and good resistance to devitrification [6, 10-11]. Because of its high molecular weight and large ionic radius of Bi^{3+}, significantly enhances density when added into B_2O_3-TeO_2 host. Depending on composition, it can also function as a network former through BiO_3 units or as a modifier through BiO_6 units [12-13]. Systematic investigations of bismuth oxide with boro-tellurite glass system established a direct correlation between glass structure, composition, and shielding efficiency. An increase in Bi_2O_3 concentration typically results in higher density and mass attenuation coefficient (MAC), along with a corresponding decrease in the half-value layer (HVL) and mean free path (MFP). Other than that, these modifications show an improvement in shielding capacity across a wide range of photon energies [5, 8]. In radiation intensive environment such as radiotherapy, medical imaging, and industrial non-destructive testing, there is a continuing need for transparent and chemical stable shiels with high effective atomic number and optimizes thickness. Tellurite and bismuth glasses meet many of these criteria because both contribute large atomic masses and strong photon interaction probabilities, while B_2O_3 provides glass-forming ability and structural flexibility [14].

Parameters such as density, molar volume, oxygen packing density, and boron-boron separation distance provide a quantitative between composition and network structure. In boro-tellurite glasses with different modifiers can shows how cation size and field strength reorganize BO_3/BO_4 and TeO_3/ TeO_4 polyhedra. Boro-tellurite glasses containing barium, display relatively low OPD but high average molecular weight, which is interpreted as a densely packed network favourable for shielding [4]. In Bi_2O_3-K_2O-ZnO-V_2O_5-B_2O_3 and Bi_2O_3-TeO_2-MgO-Na_2O_3-B_2O_3 glass system, increasing bismuth content has been reported to raises density and OPD, while reducing the average boron-boron separation, reflecting enhanced network compactness [15-16]. Therefore, combines assessment of density, molar volume and boron-boron separation is essential for a comprehensive structural evaluation of any newly design bismuth-boro-tellurite glass. The radiation shielding performance of glass materials is commonly assessed using mass attenuation coefficient (MAC), half value layer (HVL), and mean free path (MFP). MAC quantifies the probability of photon interaction per unit mass and depends strongly on effective atomic number and photon energy [17]. From MAC, practically shielding parameters such as the half value layer (HVL) and mean free path (MFP) can be derived. MFP represents the average distance travelled by a photon between successive interaction, while HVL corresponds to the thickness of materials required to reduce halve the incident photon intensity. All these parameters are strongly energy-dependent, exceeds by Compton scattering and pair production at higher energy levels, while by photoelectric absorption at low energies [14]. Lower HVL and MFP value indicate improved shielding effectiveness.

This study aimed to clarify the relationship between compositional variation, network structure, and radiation attenuation performance by comprehensively analysing of bismuth boro-tellurite glasses with varying Bi_2O_3 concentrations. Density, molar volume, oxygen packing density, and boron-boron separation measures were used to evaluate structural changes within the glass systems. These parameters provide insight into the role of Bi_2O_3 incorporation in altering network compactness and its consequent impact on shielding performance.

2.0 METHODS AND MATERIAL

Seven glass samples with composition $[(TeO_2)_{0.7}(B_2O_3)_{0.3}]_{1-x}(Bi_2O_3)x$ (where x = 0, 0.05, 0.10, 0.15, 0.20, 0.25, and 0.30 mol fraction) were prepared by using a melt-quenching technique. The raw material of boron oxide B_2O_3 (97.5% purity), tellurium (IV) dioxide TeO_2 (99.95% purity) and bismuth oxide Bi_2O_3 (99.975% purity), from Assay, Alfa Aesar were used in the preparation of these glass samples. A weighed chemical was thoroughly blended and manually ground in an alumina crucible for approximately 40 minutes until a homogenous fine powder was obtained. The mixture was then melted at 1000 °C for 60 minutes. Once a clear molten liquid was formed, it was transferred onto a preheated stainless-steel mould and subsequently annealed at 450 °C for 90 minutes to relieve internal stress. Finally, the samples were allowed to reach room temperature by natural cooling. The glass density was determined using Archimedes' principle with distilled water as the immersion fluid. Then, the density value can be determined using the following formula:

$$\rho_g = \rho_w \frac{m_{air}}{m_{air} - m_w} \quad (1)$$

*Corresponding Author | Amat, A. | azuraida@upnm.edu.my

where ρ_g represents the density of the glass sample, ρ_w is the density of water, m_{air} is the mass of the glass sample in the air, and m_w refer the mass measured while the glass sample immersed in water. While, the molar volume, V_m can subsequently be determined using the equation:

$$V_m = \frac{M}{\rho_g} \tag{2}$$

where M represent the total molecular weight [14].
In this work, to confirm the compaction of glass structure, the average boron–boron separation, d_{B-B} has been calculated using the expression:

$$\langle d_{B-B} \rangle = \left(\frac{V_m^B}{N_A}\right)^{1/3} \tag{3}$$

where N_A is Avogadro's number (6.0228×10^{23} g/mol) and V_m^B represent the partial molar volume which corresponds that contains one mole of boron within the given structure. This volume, V_m^B are determined using following relation:

$$V_m^B = \frac{V_m}{2(1 - X_B)} \tag{4}$$

where V_m is the molar volume of glass, and X_B is the molar fraction of boron oxide, B_2O_3.

The oxygen packing density (OPD) was calculated from the molar volume, V_m using the following equation:

$$OPD = \frac{1000 \times c}{V_m} \tag{5}$$

where c represents the number of oxygens per unit formula [18]. Radiation attenuation characteristics were examined using the Phy-X platform. For each glass sample, the calculated elemental weight fractions together with the corresponding measured density were supplied as input parameters. The evaluation was conducted at 0.662 MeV photon energy. Using embedded photon cross-section datasets and mixture rule calculations, the software produced energy-dependent value of mass attenuation coefficient (MAC), Half Value Layer (HVL), and Mean Free Path (MFP) for every investigated composition. Within the Phy-X environment, the attenuation behaviour of multi-component materials is estimated by summing the weighted contributions of individual element cross-sections according to their respective proportions in the glass matrix. The calculated shielding indicators therefore represent theoretical predictions based on standard photon interaction data and assume uniform elemental distribution throughout the materials.

3.0 RESULTS AND DISCUSSION

3.1 Glass Density, Molar Volume, Oxygen Packing Density, and Boron-Boron Separation

All seven glass compositions were successfully prepared using the conventional melt-quenching method, visual inspection confirm that the obtained samples were transparent and free from of visible air bubble inclusions, indicating good homogeneity. Figure 1 shows the experimental densities value of each glass samples derived using Archimedes' principles. Determining the density is important because it reflects the degree of atomic packing and matrix densification of the glass matrix, which directly influences its physical strength. The results demonstrate a clear upward trend, with the density increasing by approximately 84.5% as bismuth content progressively raised to 0.30 mol fraction. The increment value of densities because of the high atomic mass of bismuth compared to boron and tellurium. Heavy Bi^{3+} ions are progressively replacing lighter network formers, leading to a glass denser [19]. The measured density well reflected in any changes that occur inside the network structure such as expansion or compaction, coordination number, changes in cross-link density, and dimensionality of the interstitial spaces are well reflected in the measured density [20].

*Corresponding Author | Amat, A. | azuraida@upnm.edu.my

Interestingly, the molar volume, V_m of the present samples initially reduced ~ 3% from 40.88 cm^3 mol^{-1} (BTe) to 37.42 cm^3 mol^{-1} (30BiBTe) as shown in Table 1. This trend follows the inverse relationship between density and molar volume as expressed in Equation (2), where density and molar volume are inversely proportional to each other [14] the initial decrease in molar volume is attributed to enhanced structural packing due to the incorporation of Bi^{3+} ions. At higher concentrations, Bi^{3+} likely acts as a network modifier the increased rather than former. This introduces non-bridging oxygen (NBOs), causing local structural expansion despite the overall increase in density and decreased OPD indicating a reduction in the compactness of the oxide network [19, 21-22]. Table 2 show the data of molar volume, V_m, boron-boron separation distance, d_{B-B} and oxygen packing density, OPD for present glass with different amount of bismuth oxide. The reduction of non-bridging oxygen (NBOs) was confirmed further by calculation of OPD using formula in Equation 5. The OPD values remain relatively stable (0.0563-0.0707 g/cm^3), with a slight increased at low Bi_2O_3 concentration. Relatively modest variation compared with density, often decreasing as molar volume and more NBOs generated [23-24]. The boron-boron separations, d_{B-B} distance decreased systematically from 0.4270nm (BTe) to 0.3192 nm as Bi_2O_3 (30BiBTe) concentration increased. The boron-boron (B-B) separation distance is direct indicator of network compactness. A shorter B-B distance reflects a more tightly packed glass structure, where atoms are closer together, resulting in higher density. A reduction in interatomic distance limits free volume while enhancing packing efficiency, thereby improving structural compactness and improved radiation attenuation performance.

Boron atoms are being pushed closer together as bismuth enter the structure of glass. This may reflect a change the formations of more BO_4 tetrahedral units, which typically result in more condensed borate network. The previous report where addition of heavy cations converts BO_3 to more compact BO_4 groups and increases crosslinking, reducing B-B distance the conversion of BO_3 to BO_4 unit's configurations cannot be directly confirmed based on structural and density parameters [25-26]. This transformation is typically verified using spectroscopy techniques such as FTIR, Raman spectroscopy, or NMR, which provided detailed insight into the coordination environment of boron. In the present study, the observed reduction in B-B separation, together with the increase in density, indicates a more compact structure that consistent with the BO_3 to BO_4 conversion has been reported [17]. In bismuth boro-zinc glass, B-B separations in BO_3 decreased as Bi_2O_3 rises, explicitly linked to BO_3 to BO_4 transformation and structural condensation in parts of the network [26].

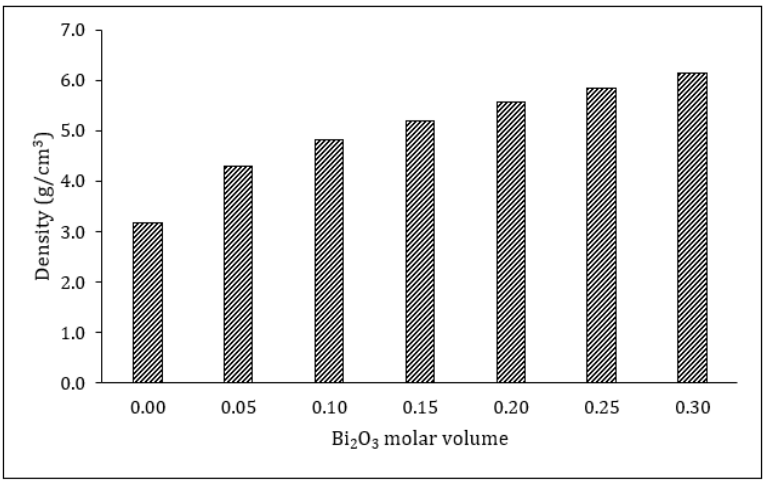

Figure 1. Graph density of present sample

Table 1. Glasses with different Bi_2O_3 concentrations (Mol fraction)

Glass Sample	Bi_2O_3 concentration	V_m (cm^3 mol^{-1})	OPD (gcm^{-3})	$\langle d_{B-B} \rangle$ (nm)
BTe	0	40.88	0.0563	0.4270
5BiBTe	0.05	33.05	0.0707	0.3416
10BiBTe	0.10	34.52	0.0687	0.3400
15BiBTe	0.15	35.24	0.0683	0.3342
20BiBTe	0.20	35.81	0.0682	0.3277
25BiBTe	0.25	36.95	0.0670	0.3237
30BiBTe	0.30	37.42	0.0671	0.3192

*Corresponding Author | Amat, A. | azuraida@upnm.edu.my

3.2 Radiation Shielding Properties

The theoretical value of mass attenuation coefficient, MAC of present glass sample was obtained using Phy-X and presented in Figure 2. The graph enlightens the relationship between MAC value and glass composition (0.00 to 0.30 mol%). At 0.662 MeV, MAC value increased from 0.075 cm^2/g at 0.00 mol% to 0.095 cm^2/g at 0.30 mol% Bi_2O_3, representing a 26.7% enhancement. The introducing of Bi_2O_3 into the glass network introduces heavier nuclei attribute to the large atomic number of Bi (Z = 83) which is substantially greater than B (Z = 5) and Te (Z = 52). The presence of these high Z elements intensifies photon-matter interactions, particularly through mechanism that are sensitive to atomic number. Consequently, increasing the Bi_2O_3 content strengthens the overall attenuation capability of the material, as reflected by the rise in mass attenuation coefficient values and the corresponding improvement in gamma-ray shielding performance [14].

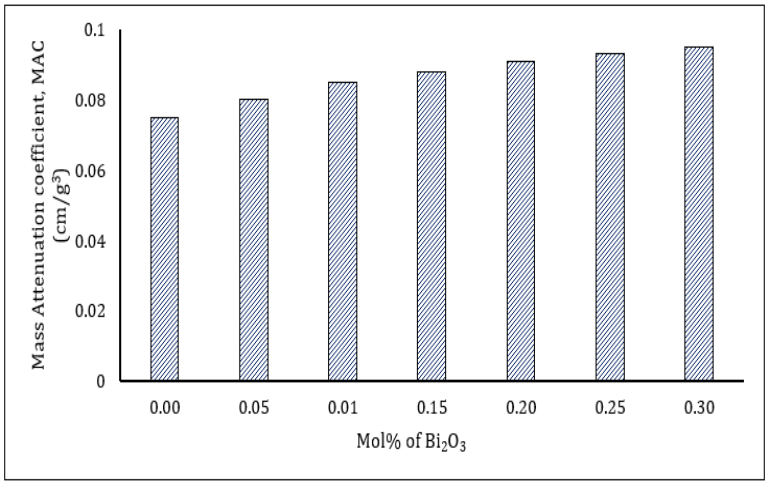

Figure 2. Graph mass attenuation coefficients, MAC of present samples at energy 0.662 MeV

At a photon energy of 0.662 MeV, the glass containing 30 mol% Bi_2O_3 exhibits a MAC value of 0.095 cm^2/g, which is slightly higher than the values reported in comparable studies, as summarized in Table 2. This modest increase indicates in an enhanced photon attenuation capability relative to previously published compositions. The improved performance can be attributed to differences in compositional design, density, effective atomic number, and structural compactness, all of which govern the probability of photon interaction within the glass matrix. Even minor variations in oxide proportions may alter the electron density and atomic packing arrangement, thereby influencing attenuation behaviour at this energy level. Overall, the obtained MAC values suggest the developed bismuth boro-tellurite glass system exhibits competitive shielding performance compared with related materials reported in the literature.

Table 2. Value of the mass attenuation coefficients of the present sample

Glass composition	MAC (cmg^{-3})	Ref
30BiBTe	0.095	Present work
$20TeO_2$+10BaO +10ZnF+ xBi_2O_3+$1Dy_2O_3$ + $(59-x)B_2O_3$	0.093	[27]
$10Li_2O$ + 20CuO + xBi_2O_3 + $(70-30)B_2O_3$	0.090	[28]
$10Bi_2O_3$-70 B_2O_3-20BaO	0.089	[29]
(70-0.5) B_2O_3–$5TeO_2$–$10Bi_2O_3$–$10SrCO_3$–$5K_2CO_3$-xEr_2O_3	0.088	[30]

The theoretical value of half value layer, HVL of present glass system at photon energy 0.662 MeV presented in Figure 3. At 0.00 mol% Bi_2O_3, the HVL is 2.91 cm, indicating that nearly 3 cm of glass thickness required to attenuate the intensity of photon energy 0.662 MeV gamma radiation by 50% of its initial value. As the composition increased, the HVL decreased systematically. This progressive reduction in HVL from 2.910 cm to 1.184 cm represents a remarkable 59.3% decreased, demonstrating the substantial improvement in radiation shielding efficiency achieved through compositional optimization. Lower HVL values indicate enhance shielding efficiency, as less material thickness is required to attenuate incident radiation to half its initial intensity. The enhance structural compactness reduces the free volume within the network, thereby increasing the probability of photon interaction [2]. Consequently, thinner glass thickness is required to attenuate 50% of incident gamma radiation, confirming that the presence of Bi_2O_3 effectively enhance the radiation attenuation efficiency of develop the glass system.

*Corresponding Author | Amat, A. | azuraida@upnm.edu.my

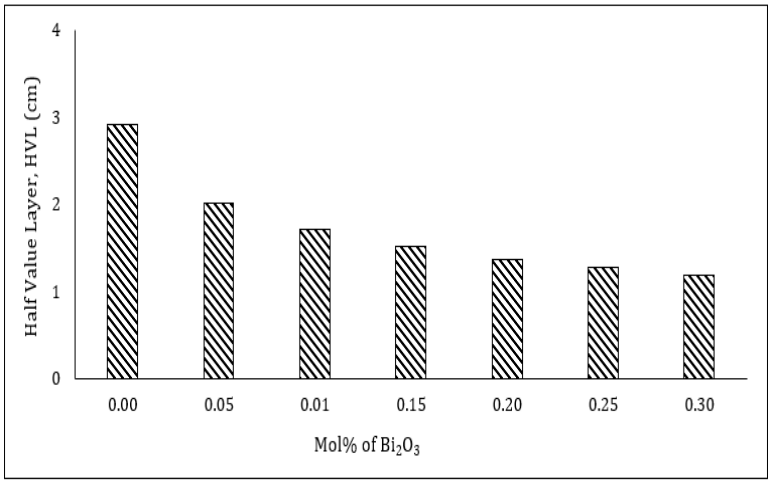

Figure 3 Graph HVL of present glasses at energy 0.662 MeV

At an energy of 0.662 MeV, the glass containing 30 mol% Bi_2O_3 recorded an HVL of 1.184 cm, which is the lowest value among the current samples as well as those listed in Table 3. In comparison, the $(59-x)B_2O_3+20TeO_2+10ZnF+10BaO + xBi_2O_3+1Dy_2O_3$ exhibit an HVL of 1.64 cm [27]. This indicates that the present composition achieves as 27.9% lower HVL (1.184 versus 1.64 cm), reflecting a notable enhancement in shielding capability. Practically, this indicates that approximately 0.456 cm less material thickness is required to attenuate halve of the incident radiation [14]. Similarly, the reported $0.9(BaO+0.5Bi_2O_3+0.5B_2O_3)$ -(1-0.9) SiO_2 (BBS) [31] exhibits an HVL of 1.27 cm. the current glass therefore provides a 68% reduction in HVL compared with the BBS system (1.184 cm versus 1.27 cm). Although the improvement over BBS is relatively moderate, the $[(TeO_2)_{0.7}(B_2O_3)_{0.3}]_{0.70}(Bi_2O_3)_{0.30}$ composition consistently demonstrates superior attenuation performance at 0.662 MeV. Overall, these findings confirm that optimizing the boro-tellurite matrix with a high Bi_2O_3 content (30 mol%) is an effective strategy for enhancing gamma radiation shielding performance.

Table 3. Comparison between the values of the half value layer of the proposed glass

Glass composition	HVL (cm)	Ref
$[(TeO_2)_{0.7}(B_2O_3)_{0.3}]_{0.70}(Bi_2O_3)_{0.30}$	1.184	Present work
$(59-x)B_2O_3+20TeO_2+10ZnF+10BaO + xBi_2O_3+1Dy_2O_3$	1.64	[27]
$0.9(BaO+0.5Bi_2O_3+0.5B_2O_3)$ -(1-0.9) SiO_2 (BBS)	1.27	[31]

The mean free path (MFP) value at 0.662 MeV for present glass series shows a decreasing pattern from 4.198 cm to 1.709 cm. MFP value follow similar trends with HVL when bismuth oxide content is increasing. The average distance of a photon travels before interaction with materials is represented by the MFP. The lower values indicate more frequent interactions and better shielding effectiveness. With increasing Bi_2O_3 incorporation, the introduction of high atomic number Bi^{3+} ions enhance the electron density and improved atomic packing within the glass system, leading to a more compact structure. The average distance that photons can travel before interacting is decreased by the denser network, which raises the probability of photon interaction over a shorter travel distance [2]. This trend indicates that Bi_2O_3 addition contributes to improved radiation shielding performance by limiting photon penetration depth within the glass system. Density is the most direct structural factor that strongly correlates with the MAC, HVL, and MFP [1, 3]. Glass density expresses how much mass were packed per unit volume. Higher density increases the number of interaction for incident photons, so the mass attenuation coefficient (MAC) generally rises, and HVL/MFP decreased [32]. The addition of Bi_2O_3 which has high atomic mass, Z into boro-tellurite glass system leads to systematic increase in density. As the density increases, the glass exhibits larger MAC values and correspondingly lower HVL and MFP at the same photon energy [33]. This behaviour confirms the direct relationship between compositional modification, density enhancement, and improved radiation shielding performance.

*Corresponding Author | Amat, A. | azuraida@upnm.edu.my

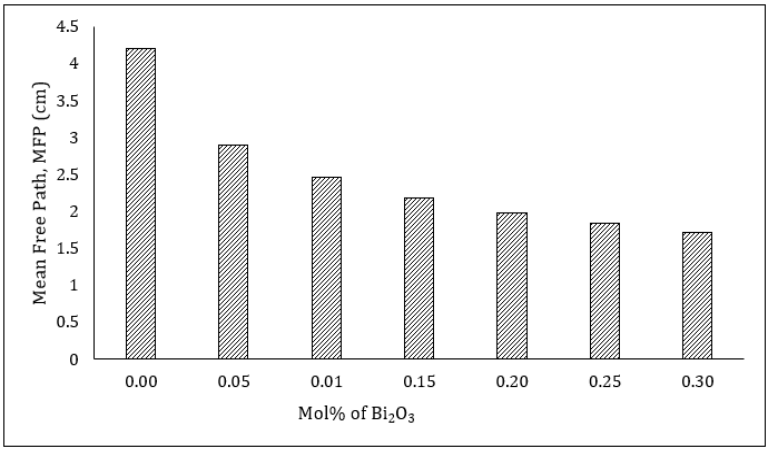

Figure 4. Graph MFP of present glasses at energy 0.662 MeV

As previously discussed, the gradual decrease in boron-boron (B-B) separation with increasing Bi_2O_3 content signifies progressive structural condensation within the glass network. The shortening of the average distance between boron units indicates that the glass framework becomes more compact, with reduced interstitial space and improved atomic packing. This structural evolution is consistent with the measured rise in density and oxygen packing density (OPD), indicating that compositional modification leads to a denser glass network configuration [34]. The impact of this structural compaction extends directly impact on the radiation attenuation behaviour. A reduced B-B separation reflects a higher atom, and electrons are closer per unit volume, effectively increasing the electron density of the material. At 0.662 MeV, where Compton scattering is the dominant photon interaction mechanism, attenuation efficiency is strongly vulnerable on electron density. Consequently, a structurally condensed network enhances the probability of photon-electron interactions, improving the overall shielding performance [35-36]. This explains the observes increment in the mass attenuation coefficient (MAC) accompanied the corresponding decrease in half-value layer (HVL) and mean free path (MFP). The structural tightening induced by Bi_2O_3 incorporation thus establishes a clear and physically meaningful connecting between microscopic network parameters and macroscopic shielding performance. Accordingly, the reduction in B-B separation across the present glass series serves as a critical structural indicator of enhance photon attenuation capability rather than merely reflecting a geometric descriptor of network arrangement.

4.0 CONCLUSIONS

All seven glasses were successfully fabricated by melt-quenching. Density increases by ~84.5% as Bi_2O_3 rises to 0.30 mol%, while B-B separation distance is reduced from 0.4270 to 0.3192 nm. The incorporation of high-Z of bismuth ions into glass network, replacing lighter B and Te species, increases the overall density of the system. This compositional substitution promotes structural compaction, driving boron units into closer proximity. This structural change directly improved the radiation shielding properties. At 0.662 MeV, the MAC value increased from 0.075 to 0.095 cm^2/g, while HVL and MFP value decreased from 2.910 cm to 1.184 cm and from 4.198 cm to 1.709 cm, respectively. The Bi_2O_3 fraction and parallel trends of MAC, HVL, and MFP with photon energy confirm that Bi-rich compositions provide more frequent photon-matter interactions and improve attenuation. The 30BiBTe glass (0.30 mol fraction Bi_2O_3) represents the optimum composition in the present glass series. It exhibits the highest density and the shortest B-B separation, accompanied by higher MAC and lower HVL and MFP. This combined structural and shielding advantages indicate that 30BiBTe is a potential lead-free candidate glass for gamma-radiation shielding applications.

5.0 CONFLICT OF INTEREST

Author declares that there is no conflict of interest regarding the publication of the paper.

6.0 AUTHORS CONTRIBUTION

Ramli, N. F (Validation; Investigation; Writing-original draft; Concept Data- analysis interpret result)
Amat, A, (Conception; Funding Acquisition; Supervision)
Yusoff W. Y. W. (Draft Manuscript preparation)
Ahmad N. (Draft Manuscript preparation)

*Corresponding Author | Amat, A. | azuraida@upnm.edu.my

7.0 ACKNOWLEDGEMENT

The author fully acknowledges ministry of higher education (MOHE) for the approved fund which makes this important research viable and effective. This research is fully supported by FRGS grant, (FRGS/1/2025/STG05/UPNM/02/1).

List of Reference

[1] Al-Buriahi, M. S., Rashad, M., Alalawi, A., & Sayyed, M. I. (2020). Effect of Bi2O3 on mechanical features and radiation shielding properties of boro-tellurite glass system. *Ceramics International, 46*(10), 16452–16458.

[2] Gaballah, M., et al. (2020). Mechanical and nuclear radiation shielding properties of different boro-tellurite glasses: A comprehensive investigation on large Bi2O3 concentration. *Physical Scrutiny, 95*(8), 085701.

[3] Kamislioglu, M. (2021). Research on the effects of bismuth borate glass system on nuclear radiation shielding parameters. *Results in Physics, 22*(3), 03844.

[4] Sasirekha, C., Komal Poojha, M. K., Marimuthu, K., & Vijayakumar, M. (2023). Investigations on physical, structural, elastic, optical and radiation shielding properties of boro-tellurite glasses for radiation waste management applications. *Optical Materials, 141*(7), 113917.

[5] Naseer, K. A., Marimuthu, K., Al-Buriahi, M. S., Alalawi, A., & Tekin, H. O. (2021). Influence of Bi2O3 concentration on barium-telluro-borate glasses: Physical, structural and radiation-shielding properties. *Ceramics International, 47*(1), 329–340.

[6] Amat, A., Mansor, I., & Saleh, H. S. (2025). Compositional impact of cerium oxide on the gamma radiation shielding properties of bismuth-boro-tellurite glass. *Journal of Advanced Research in Micro and Nano Engineering, 33*(1), 92–101.

[7] Fakhrul, M., et al. (2026). Radiation shielding study of heavy metal oxide bismuth-tungsten borate based glasses for defense and medical applications. *Journal of Advanced Research in Applied Sciences and Engineering Technology, 60*(3), 90–97.

[8] Salimov, R., et al. (2024). Simulation and calculation of the radiation attenuation parameters of newly developed bismuth boro-tellurite glass system. *Journal of Radiation Research and Applied Sciences, 17*(4), 101091.

[9] Mohamed-Kamari, H., Oo, H. M., & Wan-Yusoff, W. M. D. (2012). Optical properties of bismuth tellurite based glass. *International Journal of Molecular Sciences, 13*(4), 4623–4631.

[10] Azuraida, A., Halimah, M. K., Ishak, M., Hasnimulyati, L., & Ahmad, S. I. (2020). Gamma ray shielding parameter of barium-boro-tellurite glass. *Chalcogenide Letters, 17*(4), 187–196.

[11] El-Mallawany, R., Abou-Taleb, W. M., Naeem, M. A., Kotb, S. M., Krar, M. E., & Talaat, S. (2022). Impact of B2O3 on physical, optical characteristics and radiation attenuation factors of borotellurite glasses. *Journal of Materials Research and Technology, 18*(5), 2531–2545.

[12] Saddeek, Y. B., et al. (2018). Physical properties of B2O3–TeO2–Bi2O3 glass system. *Journal of Non-Crystalline Solids, 498*(25), 82–88.

[13] Kundu, R. S., Dhankhar, S., Punia, R., Nanda, K., & Kishore, N. (2014). Bismuth modified physical, structural and optical properties of mid-IR transparent zinc boro-tellurite glasses. *Journal of Alloys and Compounds, 587*, 66–73.

[14] Gbashi, K. R., Salih, A. T., Najim, A. A., & Muhi, M. A. (2020). Nanostructure characteristics of Bi2O3: Al2O3 thin films and the annealing temperature effect on morphological, optical, and mechanical properties. *Superlattices and Microstructures*, 146, 106656.

[15] Aloraini, D. A., Sayyed, M. I., Kumar, A., Yasmin, S., Almuqrin, A. H., Tishkevich, D. I., & Trukhanov, A. V. (2022). Studies of physical, optical, and radiation shielding properties of Bi2O3-TeO2-MgO-Na2O-B2O3 glass system. *Optik*, *268*, 169680.

[16] Bhattacharya, S., Kundu, R., Bhattacharya, K., Poddar, A., & Roy, D. (2022). Optical characterization and polaron radius of Bi2O3 doped silica borotellurite glasses. *Journal of Luminescence, 246*(6), 118868.

[17] Halimah, M. K., Azuraida, A., Ishak, M., & Hasnimulyati, L. (2019). Influence of bismuth oxide on gamma radiation shielding properties of boro-tellurite glass. *Journal of Non-Crystalline Solids, 512*(15), 140–147.

[18] Sutrisno, M. S., Sabri, N. S., & Hisam, R. (2021). Effects of Bi2O3 on DC conductivity and nonlinear optical properties of mixed ionic–electronic 98[20Li2O-xBi2O3-(80-x)TeO]-2Ag glass system. *Applied Physics A, 127*(10), 770.

*Corresponding Author | Amat, A. | azuraida@upnm.edu.my

[19] Stalin, S., Edukondalu, A., Samee, M. A., Srinivasu, C., & Rahman, S. (2020). Physical and optical investigations of Bi2O3-TeO2-B2O3-GeO2 glasses. *Materials Research Express, 6*(12), 125209.
[20] Shen, J., Lin, X., Liu, J., & Li, X. (2018). Effects of cross-link density and distribution on static and dynamic properties of chemically cross-linked polymer. *Macromolecules, 52*(1), 121–134.
[21] Singh, J., et al. (2022). Impact of ZnO on the physical and optical properties of PbO–B2O3 glasses. *Acta Physica Polonica A, 142*(2), 195–200.
[22] Ibrahim, S., Ali, A. A., & Fathi, A. M. (2024). A comprehensive investigation of Bi2O3 on the physical, structural, optical, and electrical properties of K2O.ZnO. V2O5. B2O3 glasses. *Scientific Reports, 14*(1), 58567.
[23] Hordieiev, Y. S., & Zaichuk, A. V. (2024). Preparation and characterization of strontium-doped bismuth borate glasses. *Digital Journal of Nanomaterials and Biostructures, 19*(2), 773–783.
[24] Bhemarajam, J., Prasad, P. S., Babu, M. M., Özcan, M., & Prasad, M. (2021). Investigations on structural and optical properties of various modifier oxides (MO = ZnO, CdO, BaO, and PbO) containing bismuth borate lithium glasses. *Journal of Composites Science, 5*(12), 308.
[25] Pattar, V., Rajashekara, K. M., Devaraja, C., Kaewkhao, J., Surzhikova, D. P., & Rajanavaneethakrishna, R. (2024). Investigation of structural, physical and optical properties of sodium boro-tellurite glasses doped with iron oxide. *Ceramics International, 50*(17), 30434–30444.
[26] Ahmed, S. A., Rajiya, S., Samee, M. A., Ahmmad, S. K., & Jaleeli, K. A. (2021). Density of bismuth boro zinc glasses using machine learning techniques. *Journal of Inorganic and Organometallic Polymers and Materials, 32*(3), 941–953.
[27] Keerthana, D., Naseer, K. A., Sekaran, S. A. R., Sayyed, M. I., Alqahtani, M. S., & Marimuthu, K. (2026). Comprehensive investigations on physical, structural, optical, and radiation attenuation properties of bismuth-incorporated boro-tellurite glasses. *Radiation Physics and Chemistry, 238*(1), 113153.
[28] Al-Fakeh, M. S., Saleh, E. E., & Alresheedi, F. (2023). Synthesis of novel Li2O-CuO-Bi2O3-B2O3 glasses for radiation protection: An experimental and theoretical study. *Inorganics, 11*(1), 27.
[29] Alshamari, A., et al. (2023). Gamma-ray-induced changes in the radiation shielding, structural, mechanical, and optical properties of borate, tellurite, and borotellurite glass systems modified with barium and bismuth oxide. *Optik, 281*(22), 170829.
[30] Ngaram, S. M., Hashim, S., Mohd Sanusi, M. S., Ibrahim, A., & Sayyed, M. I. (2025). Optimized physical and radiation attenuation properties of Er3+-doped strontium potassium bismuth-boro-tellurite glass systems: An experimental study. *Optical Materials, 159*(2), 116595.
[31] AbuAlRoos, N. J., Baharul Amin, N. A., & Zainon, R. (2025). Evaluation of radiation shielding characteristics of transparent barium bismuth borosilicate glasses derived from rice husk ash. *Journal of Alloys and Compounds, 1010*(1), 177950.
[32] Zakaly, H. M., Abouhaswa, A. S., Issa, S. A. M., Mostafa, M. Y. A., Pyshkina, M., & El-Mallawany, R. (2024). Synergistic optimization of physical, thermal, structural, mechanical, optical and radiation shielding characteristics in borate glasses doped with Bi2O3. *Optical Materials, 155*(9), 115815.
[33] Naseer, K. A., Marimuthu, K., Al-Buriahi, M. S., Alalawi, A., & Tekin, H. O. (2021). Influence of Bi2O3 concentration on barium-telluro-borate glasses: Physical, structural and radiation-shielding properties. *Ceramics International, 47*(1), 329–340.
[34] Maijawa, I., Musa, A., & Rogo, H. S. (2025). Investigation of the impact of Bi2O3 addition on the radiation shielding performance of Tm3+-doped borotellurite glasses via the Phy-X/PSD software. *Nexus of Future Materials, 2*(9), 632030.
[35] Alotaibi, B. M., et al. (2021). Fabrication of TeO2-doped strontium borate glasses possessing optimum physical, structural, optical and gamma ray shielding properties. *European Physical Journal Plus, 136*(4), 110798.
[36] Ngaram, S. M., Hashim, S., Mohd Sanusi, M. S., Ibrahim, A., & Sayyed, M. I. (2025). Optimized physical and radiation attenuation properties of Er3+-doped strontium potassium bismuth-boro-tellurite glass systems: An experimental study. *Optical Materials, 159*(2), 116595.

*Corresponding Author | Amat, A. | azuraida@upnm.edu.my